Feasibility study: Using Owlstone's Lonestar analyzer for the detection of acetic acid in crude oil

Technical POC: Russell Parris, Max Allsworth and Céline Lainé
Commercial POC: Steve Freshman

Executive Summary

Based on the results highlighted in this report, we are very confident that Owlstone's Lonestar analyser can detect acetic acid in crude oil. Based on this evidence, we envision a 10 min analysis time, giving the desired threshold limit of detection of 1 $ppm_{(w/w)}$. It has also been demonstrated that in a range of water content up to 5 $\%_{(w/w)}$in Eagle Ford crude oil, it would still be possible to detect and alarm to 1 $ppm_{(w/w)}$ of acetic acid, as the variation caused is significantly less than the acetic acid signal increase over background. For the purposes of this feasibility study, we were able to meet the 1 ppm threshold limit of detection in six crude oil types, 5 $ppm_{(w/w)}$ in two oils and 7.5 $ppm_{(w/w)}$ in one oil. Based on our extensive sampling experience and these initial results, we are convinced that with minor tweaks to the sample preparation and sample mixing (in preparation for a broader rollout/deployment of the analyser and the application) that the lower limit of detection to 1 $ppm_{(w/w)}$ can be achieved in all crude oil types.

Introduction

This body of work explores the feasibility of using Owlstone's Lonestar analyzer and its FAIMS (field asymmetric ion mobility spectrometry)-based platform for the threshold detection (<1ppm) of acetic acid (CAS 64-19-7) in crude oil. Please see Appendix C for a more in depth description of the FAIMS technology. The oil samples used in this study are presented in Table 1.The Lonestar was optimised for acetic acid detectionusing2 crude oils (highlighted in red) which represent the largest range of variability (i.e. API/ heavy sour to light sweet). Following this, the Eagle Ford crude oil was used to evaluate the effect of the crude oil water content on the acetic acid response. Finally, the optimised method was used to determine threshold concentration in the remaining seven crude oil samples.

Crude oil	API gravity	density	Sulphur content (wt%) < 0.7 % sweet > 0.7 % sour	TAN (mg KOH/g)
Eagle Ford	57	light	0.13	0.03
Peace River	15 - 20	heavy	5.00	2.45
Bakken crude	38-40	light	0.2	0.7
Permian condensate	32-41	light	n/a	n/a
Scotford AHS (Albian Heavy Synthetic)	18.9	heavy	2.38	0.43
Scotford PAS (Premium Albian Synthetic)	30.6	medium	0.05	n/a
Sun B LLS (Louisiana Light Sweet)	n/a	light	n/a	n/a
Jay crude	n/a	n/a	n/a	n/a
May crude	n/a	n/a	n/a	n/a

Table 1: Crude oil samples.

Method

A 1000 $ppm_{(w/w)}$ stock solution of commercially available glacial acetic acid (CAS 64-19-7, Sigma Aldrich, UK) was prepared in absolute ethanol (CAS 8024-45-1, Sigma Aldrich, UK). Lower concentration standards were prepared by diluting the stock solution to the desired concentrations and shaken vigorously for 5 seconds. All samples were analysed using the instrument configuration presented in Figure 1.

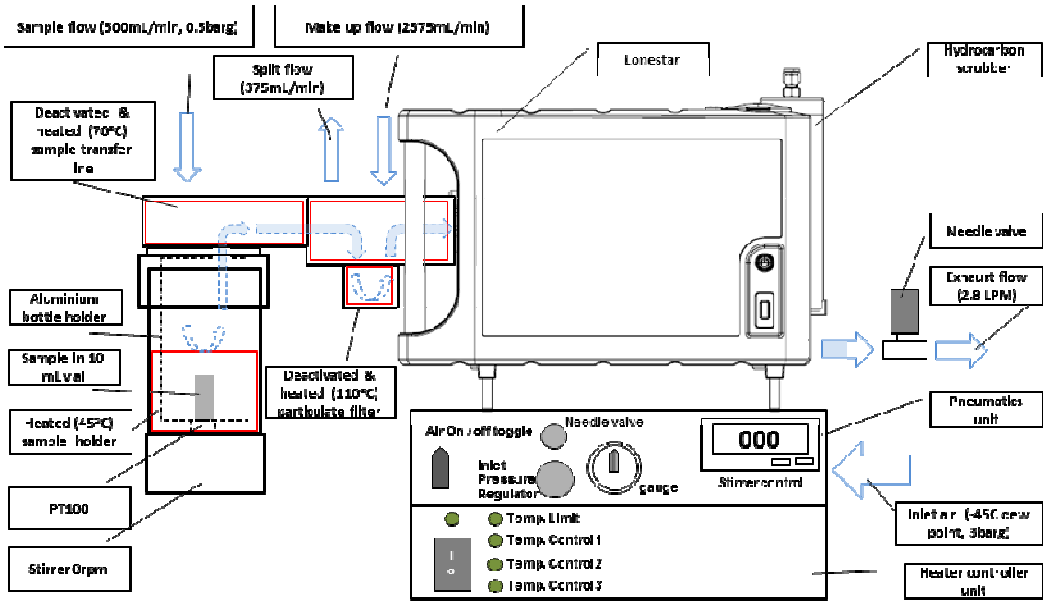

Figure 1: Experimental schematic - The Lonestar system is connected to a headspace sampling interface (left) in which sample vials (trace clean) can be mounted allowing all the environmental conditions at the sample to be controlled. The crude oil sample to be analysed is placed in the vial, the system flushes air (blue arrows) through the sample headspace and into the analyser via a particulate filter. A split flow and an additional make up flow are added to give additional dilution.

Results

Acetic acid in Eagle Ford and Peace River crude oils

Using default instrument settings, the Lonestar response was characterized for 1 and 10ppm$_{w/w}$ acetic acid standards in Eagle Ford and Peace River crude oils, providing proof of principle for the viability of this application across a large range of crude oil types.

To characterize the acetic acid response, 10ppm$_{w/w}$ acetic acid standards were prepared and analyzed using a full dispersion field (DF) sweep from 0-100% DF. An example of DF matrices for 10ppm$_{w/w}$ acetic acid in Eagle Ford crude oil is shown in Figure 2. The blue spectrum plot highlights chemicals found in the positive mode while the red spectrum illustrates the presence of chemicals identified by their negative mode response. Please refer to Appendix C for a complete description on the principles of ionization and why certain chemicals are detected in the positive or negative mode.
These full DF matrices are used to determine what % DF will be used for the acetic acid detection which is usually based on a compromise between selectivity and sensitivity. From the data collected it was decided to use 67% DF. Figure 3shows the compensation voltage (CV) spectrum taken at 67 % DF for both Eagle Ford and Peace River 10ppm$_{w/w}$ acetic acid standards. The acetic acid response at -1.94 V CV is clearly visible when compared to the 0ppm crude oil samples.

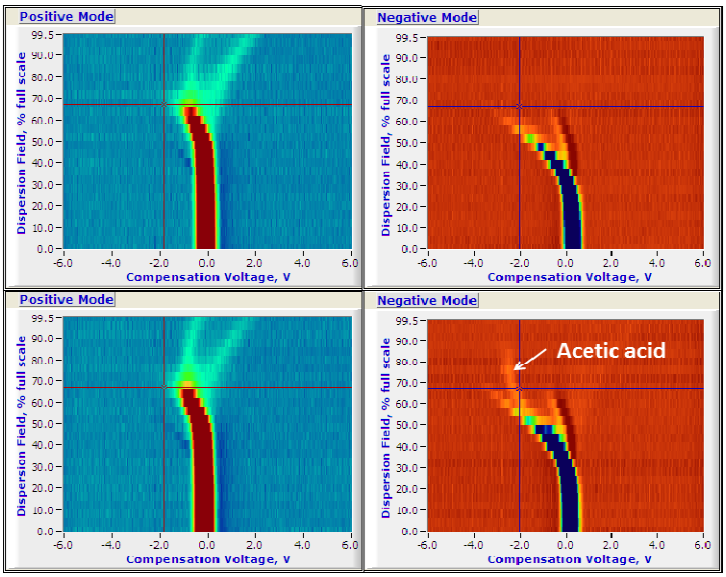

Figure 2:Dispersion field matrices of 0ppm (top) and 10 ppm$_{w/w}$ (bottom) acetic acid in Eagle Ford.

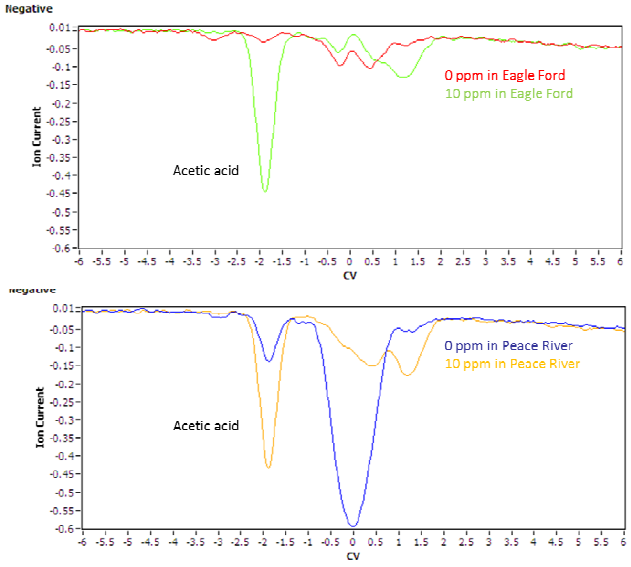

Figure 3: CV spectrum at 67% DF for 0ppm and 10ppm$_{w/w}$ acetic acid in both Eagle Ford (top) and Peace River (bottom) crude oils.

With the acetic acid peak location known, three samples were prepared for Eagle Ford and Peace River at each concentration of 0, 1 and 10ppm$_{w/w}$ acetic acid. These were then analysed by the Lonestar and the acetic acid response at 67% DF -1.94V CV is presented in Figure 4. From this figure a clear increase in ion current can be seen at the 1ppm$_{w/w}$ level when compared to the 0 ppm level for both crude oils, proving that the threshold detection level was possible across a large range of crude oil types. The next step was to optimise the instrument parameters for the 1ppm$_{w/w}$ acetic acid signal.

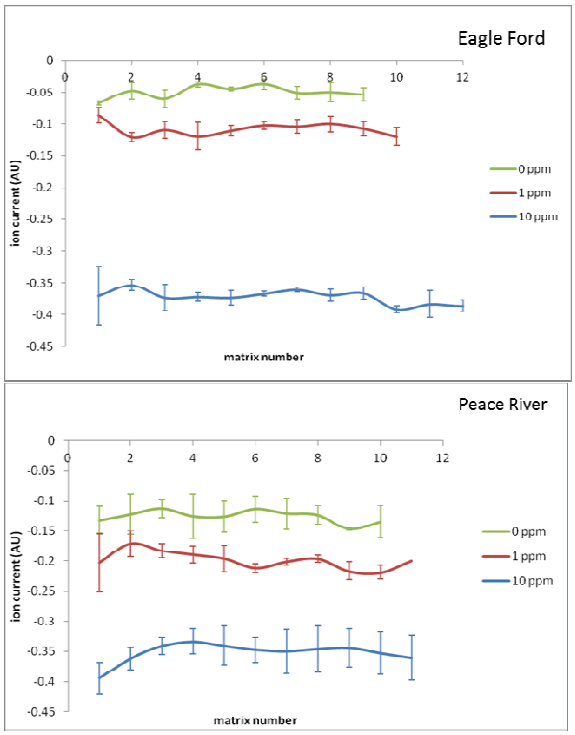

Figure 4: 0, 1 and 10ppm$_{w/w}$ acetic acid responses for subsequent matrix scans (time) for Eagle Ford and Peace River crude oils.

Method optimisation

Using 1ppm$_{w/w}$ Eagle Ford crude oil standards, the method parameters were optimized for sensitivity and analysis time, resulting in an increase in acetic acid ion current of 0.1 A.U. and an analysis time of 10min (600s).

With a known CV peak location of -1.94V using a 67%DF, the Lonestar configuration file was optimised. It only acquires data at 67%DF allowing for a higher number of scans and subsequent averaging to reduce the noise background and improve the acetic acid limit of detection. Two Eagle Ford standards containing 1ppm$_{w/w}$ acetic acid were used for this study presented against the 0 ppm concentration in

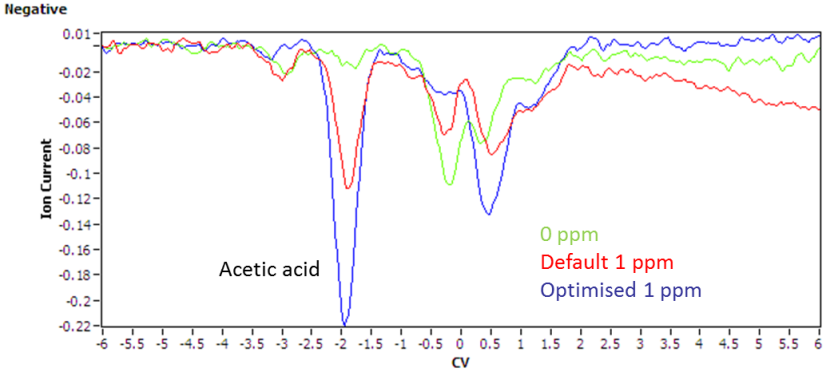

Figure *5*. The optimised Lonestar configuration gave an increase in acetic acid response to -0.22 A.U. ion current.

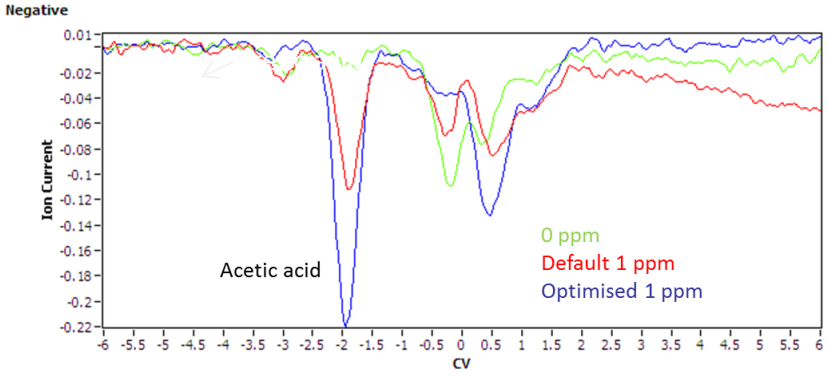

Figure 5:CV spectrum showing the 1 ppm$_{w/w}$ acetic acid response at -1.94V for the default method (red) and optimised method (blue).

Using this Lonestar configuration, 1ppm$_{w/w}$ acetic acid in Eagle Ford was analysed for 20 min to establish the optimum analysis time. Figure 6 shows a stable acetic acid response between 400 and 1000s with a realistic analysis of 600s (10min) being achievable.

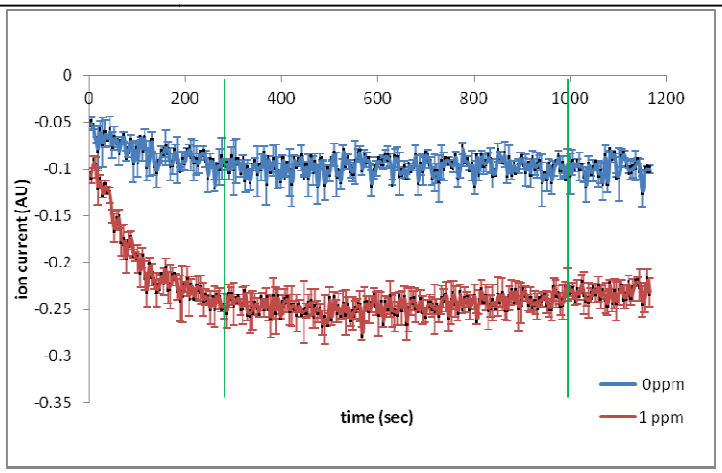

Figure 6: Three repeats of 0 and 1 ppm$_{w/w}$ acetic acid in Eagle Ford showing the stable response between 300 and 1000s (between green lines).

Acetic acid in Eagle Ford Calibration

The instrument was calibrated to ensure the 1ppm$_{(w/w)}$acetic acid response was within the linear range.

Eagle Ford crude oil samples were prepared from the 1000 ppm$_{(w/w)}$ acetic acid stock in absolute ethanol. Monitoring of the CV spectrum peak at-1.94± 0.02 V DF 67 % allows a trend of increased ion current with increased acetic acid concentration to be observed (Figure 7).

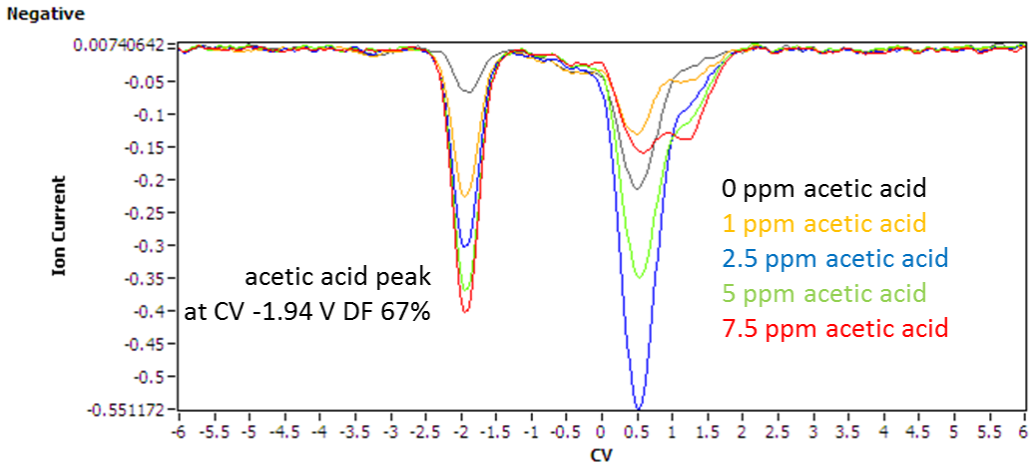

Figure 7: Raw crude data showing the CV spectra taken at 67% DF. The acetic acid peak is indicated at -1.94 V in the CV spectrum and can be seen to increase in ion current with concentration.

The acetic acid response over time is used to create a calibration curve. For each concentration, the ion current between 400 and 1000 s is averaged. A logarithmic response (r^2 = 0.985) to acetic acid concentration in crude oil is observed over a 0 to 7.5 ppm$_{(w/w)}$ range (Figure 8).

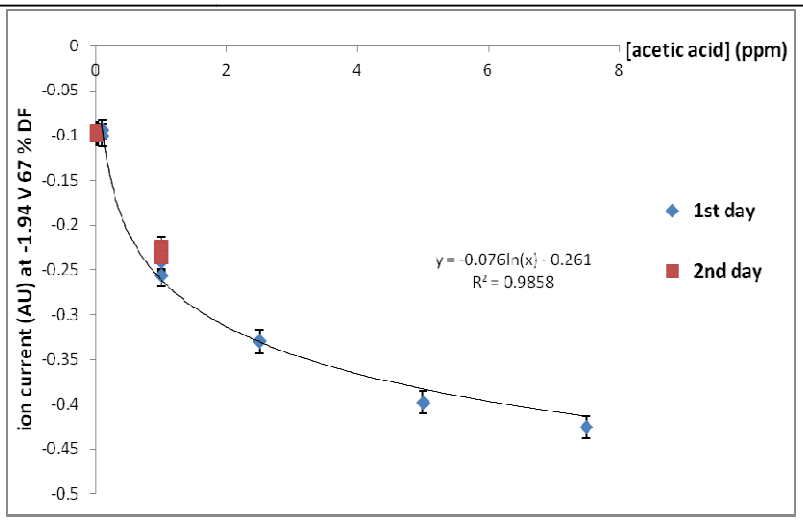

Figure 8: Calibration curve showing the detection of acetic acid in Eagle Ford crude oil over a 0 to 7.5 ppm$_{(w/w)}$ range and on two different days.

Evaluating the effect of crude oil water content on acetic acid response

Eagle Ford samples were spiked with various amounts of water from 0.1 to 5%$_{(w/w)}$and shaken vigorously for 5 s. The acetic acid was then added to create the 1ppm$_{(w/w)}$ standards to be analysed by the Lonestar.

Figure 9 shows 0 ppm acetic acid (blue) and 1 ppm$_{(w/w)}$ (red) in Eagle Ford with the presence of 0, 0.1, 0.2, 0.5, 1, 2 and 5 %$_{(w/w)}$water.

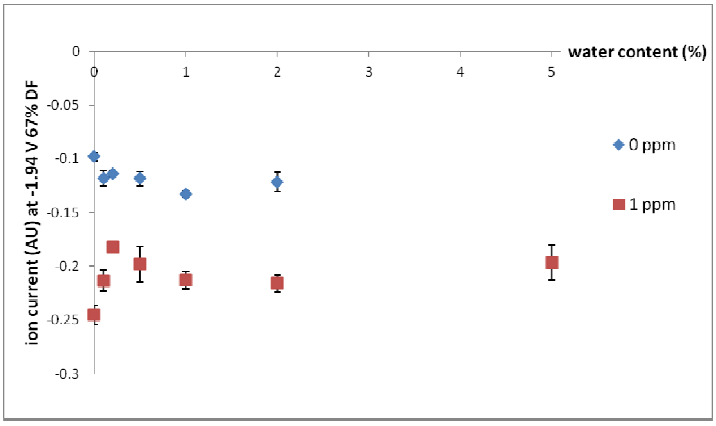

Figure 9: Effect of water on acetic acid detection in Eagle Ford crude oil. Error bars represent the standard deviation on triplicates.

The Eagle Ford crude oil background ion current remains unchanged in presence of 0.1 to 2%$_{(w/w)}$ water (blue).

For 1 ppm$_{(w/w)}$ acetic acid in Eagle Ford crude oil (red), the addition of water up to 0.2 %$_{(w/w)}$ changes the acetic acid detection by 0.07 A.U. and this quickly stabilises as the water content increases up to 5 %$_{(w/w)}$.As the difference between the 0 and 1 ppm$_{(w/w)}$signals is almost twice, an alarm threshold could still be set to detect the 1 ppm$_{(w/w)}$acetic acid concentration across this water content range.

Acetic acid limit of detection (LOD) for the remaining seven crude oils

The method was transferred to the remaining seven crude oil types to determine the acetic acid limit of detection. The detection threshold is defined as three times the standard deviation of the noise background taken from the 0 ppm standards. This can be compared to the 1 $ppm_{w/w}$ acetic acid ion current to determine if detection at this level is possible.

Table 2shows the results for the acetic acid limit of detection in the seven crude oils. The acetic acid detection of 1$ppm_{w/w}$ is possible for Bakken crude, Permian Condensate, Scotford PAS and Jay crude, in addition to Eagle Ford and Peace River. Acetic acid can be detected at 5$ppm_{w/w}$ for Sun B LLS and May crude and 7$ppm_{w/w}$ Scotford AHS.

Crude oil	0 ppm AVERAGE	0 ppm 3xSTDEV	Detection threshold (LOD ion current (AU) = AVERAGE + 3x STDEV)	1 ppm AVERAGE	5 ppm AVERAGE	7.5 ppm AVERAGE
Bakken crude	-0.06	-0.02	-0.08	-0.17 ± 0.01		
Permian condensate	-0.06	-0.03	-0.09	-0.22 ± 0.02		
Scotford PAS	-0.04	-0.03	-0.07	-0.21 ± 0.03		
Jay crude	-0.05	-0.03	-0.08	-0.22 ± 0.01		
Sun B LLS	-0.07	-0.04	-0.11	-0.10 ± 0.01	-0.20 ± 0.01	
May crude	-0.06	-0.02	-0.08	-0.07	-0.12 ± 0.01	
Scotford AHS	-0.06	-0.03	-0.09	-0.07 ± 0.01		-0.14 ± 0.01

Table 2: 1 $ppm_{w/w}$ acetic acid limit of detection in crude oil.

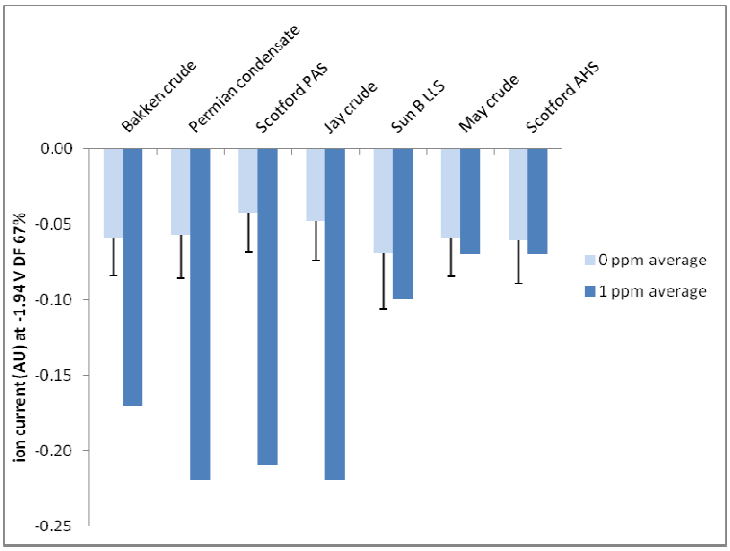

Figure 10: 1 $ppm_{w/w}$ acetic acid detection in the remaining 7 crude oil types–Error bars correspond to three times the standard deviation of the noise background taken from the 0 ppm.

Figure 10 is a plot of the 1ppm$_{w/w}$ acetic acid response for the seven crude oilsagainst the 0ppm$_{w/w}$ ion current (3x STDEV of the noise). It shows that there is a significant drop in the acetic acid response for the three crude oils that did not hit the 1ppm$_{w/w}$ detection. This could be indicative of issues in standard preparation and mixing. Therefore, we are very confident that further optimisation on this sample preparation procedure will lead to the 1 ppm$_{(w/w)}$ detection across all the crude oil types.

Conclusion

Based on the results highlighted in this report, we are very confident that Owlstone's Lonestar analyser can detect acetic acid in crude oil. Based on this evidence, we envision a 10 min analysis time, giving the desired threshold limit of detection of 1 ppm$_{(w/w).}$ It has also been demonstrated that in a range of water content up to 5 %$_{(w/w)}$in Eagle Ford crude oil, it would still be possible to detect and alarm to 1 ppm$_{(w/w)}$ of acetic acid, as the variation caused is significantly less than the acetic acid signal increase over background. For the purposes of this feasibility study, we were able to meet the 1 ppm threshold limit of detection in six crude oil types, 5 ppm$_{(w/w)}$ in two oils and 7.5 ppm$_{(w/w)}$ in one oil. Based on our extensive sampling experience and these initial results, we are convinced that with minor tweaks to the sample preparation and sample mixing (in preparation for a broader rollout/deployment of the analyser and the application) that the lower of detection to 1 ppm$_{(w/w)}$ can be achieved in all crude oil types.

Appendix A: Generating Calibration Standards with the OVG-4

Calibration standards can be generated using permeation tubes and Owlstone's OVG-4 Calibration Gas Generator. The permeation tubes are gravimetrically calibrated to NIST traceable standards. For this study an acetaldehyde permeation source was used as a confidence check to ensure that the Lonestar was operating within defined parameters.

BENEFITS

- High number of available analyte compounds, including solids and liquids as well as gases
- Easy generation of multi-component mixtures using combinations of tubes
- Cost savings by elimination of multiple expensive gas cylinders
- Reduced risk of exposure to dangerous chemicals due to small quantities used
- Fast and easy sample replacement
- Elimination of hazards associated with high pressure cylinders
- Quick and easy to set up and generate blended gas mixtures
- Adjustable concentration levels from ppm to ppb
- High accuracy and precision, even at the lowest concentrations
- Superior long term stability and repeatability*
- Portable, with compact footprint
- Easily integrated with the Owlstone Humidity Generator (OHG) for realistic environmental testing

**Owlstone offers an optional service for regular validation and instrument calibration*

The Owlstone OVG-4 is a system for generating NIST traceable chemical and calibration gas standards. It is easy to use, cost-effective and compact and produces a very pure, accurate and repeatable output.

The very precise control of concentration levels is achieved using permeation tube technology, eliminating the need for multiple gas cylinders and thus reducing costs, saving space and removing a safety hazard. Complex gas mixtures can be accurately generated through the use of multiple tubes.

By swapping out permeation tubes the OVG-4 can be used to generate over 500 calibration standards to test and calibrate almost any gas sensor, instrument or analyzer, including FTIR, NDIR, Raman, IMS, GC, GC/MS.

Current customers include – SELEX GALILEO, US Army, US Air Force, US Defense Threat Reduction Agency, Home Office Scientific Development Branch, DSTL, Commissariat à l'Énergie Atomique, EADS, United Technologies, Alphasense, Xtralis, LGC, Genzyme, IEE, Institut de la Corrosion, Rutherford Appleton Laboratory, University of Cambridge, Cranfield University among others.

Appendix B: Adding Precision Humidity with the Owlstone OHG-4 Humidity Generator

The OVG-4 can be integrated with the OHG-4 Humidity Generator to create realistic humidified test atmospheres for more realistic testing. Within this study the hygrometer was used to provide accurate inline humidity monitoring of the sample introduction line.

Appendix C: FAIMS Technology at a Glance

Field asymmetric ion mobility spectrometry (FAIMS), also known as differential mobility spectrometry (DMS), is a gas detection technology that separates and identifies chemical ions based on their mobility under a varying electric field at atmospheric pressure.Figure 11 is a schematic illustrating the operating principles of FAIMS.

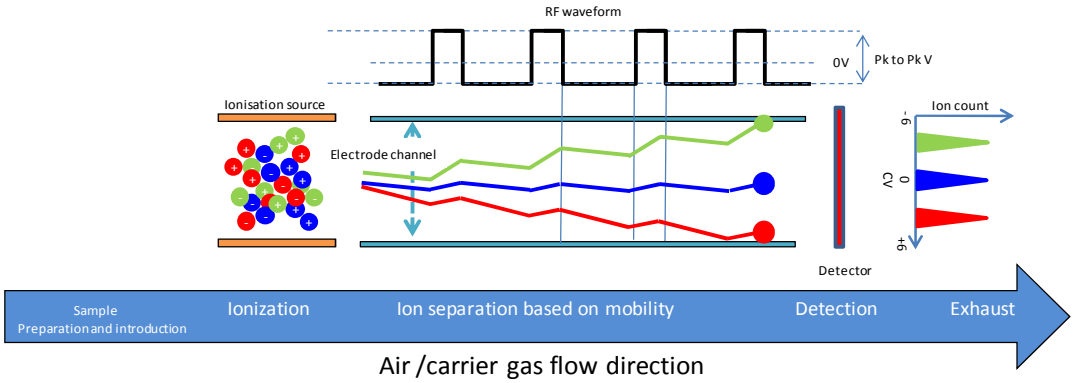

Figure 11 FAIMS schematic. The sample in the vapour phase is introduced via a carrier gas to the ionisation region, where the components are ionised via a charge transfer process or by direct ionisation, dependent on the ionisation source used. It is important to note that both positive and negative ions are formed. The ion cloud enters the electrode channel, where an RF waveform is applied to create a varying electric field under which the ions follow different trajectories dependent on the ions' intrinsic mobility parameter. A DC voltage (compensation voltage) is swept across the electrode channel shifting the trajectories so different ions reach the detector, which simultaneously detects both positive and negative ions. The number of ions detected is proportional to the concentration of the chemical in the sample

Sample preparation and introduction

FAIMS can be used to detect volatiles in aqueous, solid and gaseous matrices and can consequently be used for a wide variety of applications. The user requirements and sample matrix for each application define the sample preparation and introduction steps required. There are a wide variety of sample preparation, extraction and processing techniques each with their own advantages and disadvantages. It is not the scope of this overview to list them all, only to highlight that the success of the chosen application will depend heavily on this critical step, which can only be defined by the user requirements.

There are two mechanisms of introducing the sample into the FAIMS unit: discrete sampling and continuous sampling. With discrete sampling, a defined volume of the sample is collected by weighing or by volumetric measurement via a syringe, or passed through an adsorbent for pre-concentration, before it is introduced into the FAIMS unit. An example of this would be attaching a sample container to the instrument containing a fixed volume of sample. A carrier gas (usually clean dry air) is used to transfer the sample to the ionization region. Continuous sampling is where the resultant gaseous sample is continuously purged into the FAIMS unit and either is

diluted by the carrier gas or acts as the carrier gas itself. For example, continuously drawing air from the top of a process vat.

The one key requirement for all the sample preparation and introduction techniques is the ability to reproducibly generate and introduce a headspace (vapor) concentration of the target analytes that exceeds the lower limits of detection of the FAIMS device.

Carrier Gas

The requirement for a flow of air through the system is twofold: Firstly to drive the ions through the electrode channel to the detector plate and secondly, to initiate the ionization process necessary for detection.

As exhibited in Figure 12, the transmission factor (proportion of ions that make it to the detector) increases with increasing flow. The higher the transmission factor, the higher the sensitivity. Higher flow also results in a larger full width half maximum (FWHM) of the peaks, however, decreasing the resolution of the FAIMS unit (see Figure 13).

The air/carrier gas determines the baseline reading of the instrument. Therefore, for optimal operation it is desirable for the carrier to be free of all impurities (<0.1 ppm methane) and the humidity to be kept constant. It can be supplied either from a pump or compressor, allowing for negative and positive pressure operating modes.

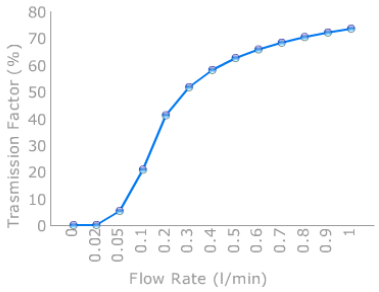

Figure 12Flow rate vs. ion transmission factor

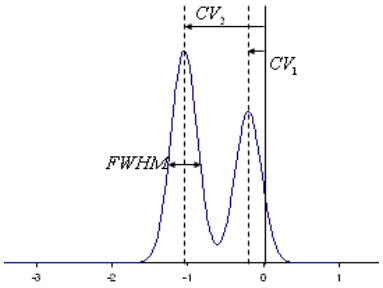

Figure 13 FWHM of ion species at set CV

Ionisation Source

There are three main vapor phase ion sources in use for atmospheric pressure ionization: radioactive nickel-63 (Ni-63), corona discharge (CD) and ultra-violet radiation (UV). A comparison of ionization sources is presented in Table 3.

Ionisation Source	Mechanism	Chemical Selectivity
Ni^{63} (beta emitter) creates a positive / negative RIP	Charge transfer	Proton / electron affinity
UV (Photons)	Direct ionisation	First ionisation potential
Corona discharge (plasma) creates a positive / negative RIP	Charge transfer	Proton / electron affinity

Table 3 FAIMS ionisation source comparison

Ni-63 undergoes beta decay, generating energetic electrons, whereas CD ionization strips electrons from the surface of a metallic structure under the influence of a strong electric field. The electrons generated from the metallic surface interact with the carrier gas (air) to form stable intermediate ions called the reactive ion peak (RIP) with positive and negative charges. These RIP ions then transfer their charge to neutral molecules through collisions thus both Ni-63 and CD are known as indirect ionization methods.

For the positive ion formation:

$N_2 + e^- \rightarrow \mathbf{N_2^+} + e^-$ (primary) + e^- (secondary)
$\mathbf{N_2^+} + 2N_2 \rightarrow \mathbf{N_4^+} + N_2$
$N_4+ + H_2O \rightarrow 2N_2 + \mathbf{H_2O^+}$
$H_2O+ + H_2O \rightarrow \mathbf{H_3O^+} + OH$
$H_3O+ + H_2O + N_2 \leftrightarrow \boldsymbol{H^+(H_2O)_2} + N_2$
$H^+(H_2O)_2 + H_2O + N_2 \leftrightarrow \boldsymbol{H^+(H_2O)_3} + N_2$

For the negative ion formation:

$O_2 + e^- \rightarrow \mathbf{O_2^-}$
$B + H_2O + \mathbf{O_2^-} \leftrightarrow \boldsymbol{O_2^-(H_2O)} + B$
$B + H_2O + O_2^-(H_2O) \leftrightarrow \boldsymbol{O_2^-(H_2O)_2} + B$

The water based clusters (hydronium ions) in the positive mode (blue) and hydrated oxygen ions in the negative mode (red), are stable ions which form the RIPs. When an analyte (M) enters the RIP ion cloud, it can replace one or (dependent on the analyte) two water molecules to form a monomer ion or dimer ion respectively, reducing the number of ions present in the RIP.

Monomer Dimer

$$H^+(H_2O)_3 + M + N_2 \leftrightarrow M\boldsymbol{H^+(H_2O)_2} + N_2 + H_2O \leftrightarrow M_2\boldsymbol{H^+(H_2O)_1} + N_2 + H_2O$$

Dimer ion formation is dependent on the analyte's affinity to charge and its concentration. This is illustrated in Figure 14 using dimethyl methylphsphonate (DMMP). Plot A shows that the RIP decreases with an increase in DMMP concentration as more of the charge is transferred over to the DMMP. In addition the monomer ion decreases as dimer formation becomes more favourable at the higher concentrations. This is shown more clearly in plot B, which plots the peak ion current of both the monomer and dimer at different concentration levels.

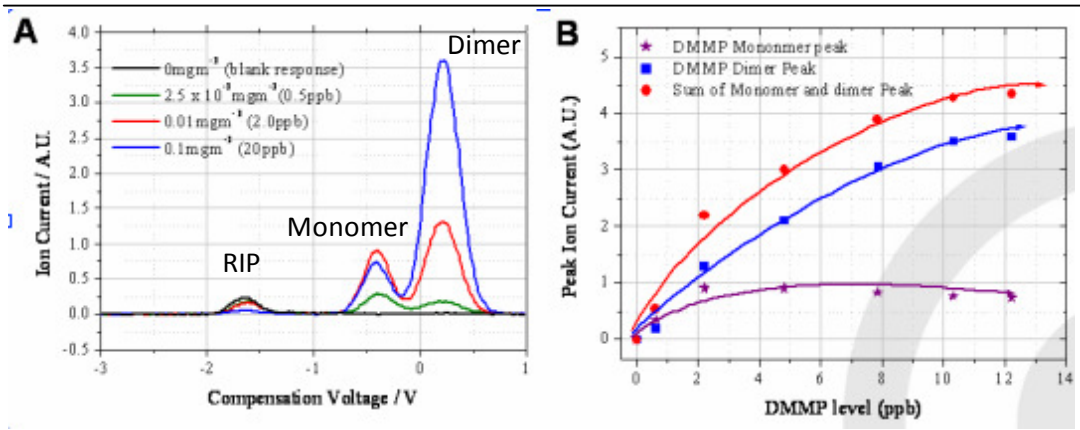

Figure 14 DMMP Monomer and dimer formation at different concentrations

the likelihood of ionization is governed by the analyte's affinity towards proton and electrons (Table 4 and Table 5 respectively).

In complex mixtures where more than one chemical is present, competition for the available charge occurs, resulting in preferential ionization of the compounds within the sample. Thus the chemicals with high proton or electron affinities will ionize more readily than those with a low proton or electron affinity. Therefore the concentration of water within the ionization region will have a direct effect on certain analytes whose proton / electron affinities are lower.

Chemical Family	Example	Proton affinity
Aromatic amines	Pyridine	930 kJ/mole
Amines	Methyl amine	899 kJ/mole
Phosphorous Compounds	TEP	891 kJ/mole
Sulfoxides	DMS	884 kJ/mole
Ketones	2- pentanone	832 kJ/mole
Esters	Methly Acetate	822 kJ/mole
Alkenes	1-Hexene	805 kJ/mole
Alcohols	Butanol	789 kJ/mole
Aromatics	Benzene	750 kJ/mole
Water		691 kJ/mole
Alkanes	Methane	544 kJ/mole

Table 4 Overview of the proton affinity of different chemical families

Chemical Family	Electron affinity
Nitrogen Dioxide	3.91eV
Chlorine	3.61eV
Organomercurials	
Pesticides	
Nitro compounds	
Halogenated compounds	
Oxygen	0.45eV
Aliphatic alcohols	
Ketones	

Table 5 Relative electron affinities of several families of compounds

The UV ionization source is a direct ionization method whereby photons are emitted at energies of 9.6, 10.2, 10.6, 11.2, and 11.8eV and can only ionize chemical species with a first ionization potential less than the emitted energy. Important points to note are that there is no positive mode RIP present when using this ionization source and also using UV ionization is very selective for certain compounds.

Mobility

Ions in air under an electric field will move at a constant velocity proportional to the electric field. The proportionality constant is known as mobility. Referring to Figure 16, as the ions enter the electrode channel the applied RF voltages create oscillating regions of high ($+V_{HF}$) and low ($-V_{HF}$) electric fields as the ions move through the channel. The difference in the ion's mobility at the high and low electric field regimes dictates the ion's trajectory through the channel. This phenomenon is referred to as differential mobility. The physical parameters of a chemical ion that affect its differential mobility are its collision cross section and ability to form clusters within the high / low regions. The environmental factors within the electrode channel affecting the ion's differential mobility are electric field, humidity, temperature and gas density (pressure).

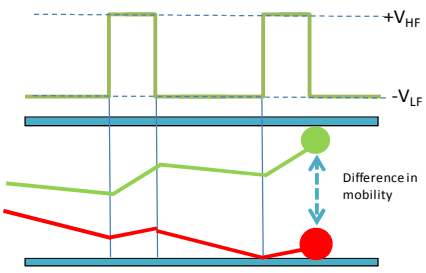

Figure 16 Schematic of a FAIMS channel showing the difference in the ions' trajectories caused by their different mobilities experienced at high and low electric fields

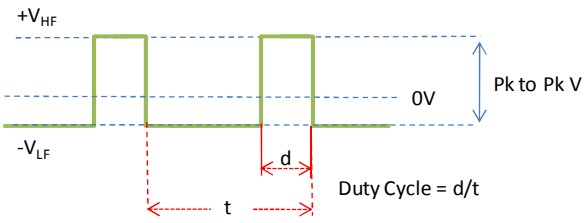

Figure 15 Schematic of the ideal RF waveform, showing the duty cycle and peak to peak voltage (Pk to Pk V)

The electric field in the high/low regions is supplied by the applied RF voltage waveform (Figure 15). The duty cycle is the proportion of time spent within each region per cycle. Increasing the peak-to-peak voltage increases / decreases the electric field experienced in the high / low field

regions and therefore influences the velocity of the ion accordingly. It is this parameter that has the greatest influence on the differential mobility exhibited by the ion.

It has been shown that humidity has a direct effect on the differential mobility of certain chemicals, by increasing / decreasing the collision cross section of the ion within the respective low / high field regions. This addition and subtraction of water molecules is referred to as clustering and de-clustering. Increased humidity also increases the number of water molecules involved in a cluster ($MH^+(H_2O)_2$) formed in the ionisation region. When this cluster experiences the high field in between the electrodes the water molecules are forced away from the cluster reducing the size (MH^+), this is known as de-clustering. As the low field regime returns so do the water molecules to the cluster, thus increasing the ion's size (clustering) and giving the ion a larger differential mobility.

Gas density and temperature can also affect the ion's mobility by changing the number of ion-molecule collisions and changing the stability of the clusters, influencing the amount of clustering and de-clustering.

Changes in the electrode channel's environmental parameters will change the mobility exhibited by the ions. Therefore it is advantageous to keep the gas density, temperature and humidity constant when building detection algorithms based on an ion's mobility as these factors would need to be corrected for. However, it should be kept in mind that these parameters can also be optimized to gain greater resolution of the target analyte from the background matrix, during the method development process.

Detection and Identification

As ions with different mobilities travel down the electrode channel, some will have trajectories that will result in ion annihilation against the electrodes, whereas others will pass through to hit the detector. To filter the ions of different mobilities onto the detector plate a compensation voltage (CV) is scanned between the top and bottom electrode (see Figure 17). This process realigns the trajectories of the ions to hit the detector and enables a CV spectrum to be produced.

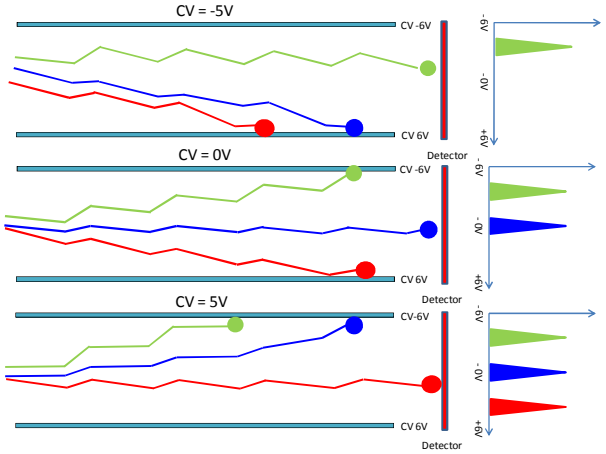

Figure 17 Schematic of the ion trajectories at different compensation voltages and the resultant FAIMS spectrum

The ion's mobility is thus expressed as a compensation voltage at a set electric field. Figure 18 shows an example CV spectrum of a complex sample where a de-convolution technique has been employed to characterize each of the compounds.

Changing the applied RF peak-to-peak voltage (electric field) has a proportional effect on the ion's mobility. If this is increased after each CV spectrum, a dispersion field matrix is constructed. Figure 19 shows two examples of how this is represented; both are negative mode dispersion field (DF) sweeps of the same chemical. The term DF is sometimes used instead of electric field. It is expressed as a percentage of the maximum peak-to-peak voltage used on the RF waveform. The plot on the left is a waterfall image where each individual CV scan is represented by compensation voltage (x-axis), ion current (y-axis) and electric field (z-axis). The plot on the right is the one that is more frequently used and is referred to as a 2D color plot. The compensation voltage and electric field are on the x, and y axes and the ion current is represented by the color contours.

P6

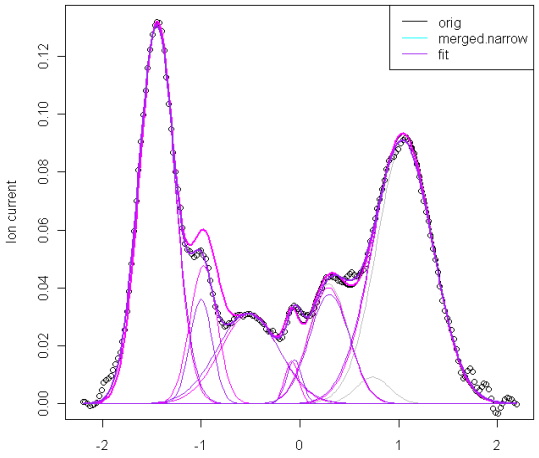

Figure 18 Example CV spectra. Six different chemical species with different mobilities are filtered through the electrode channel by scanning the CV value

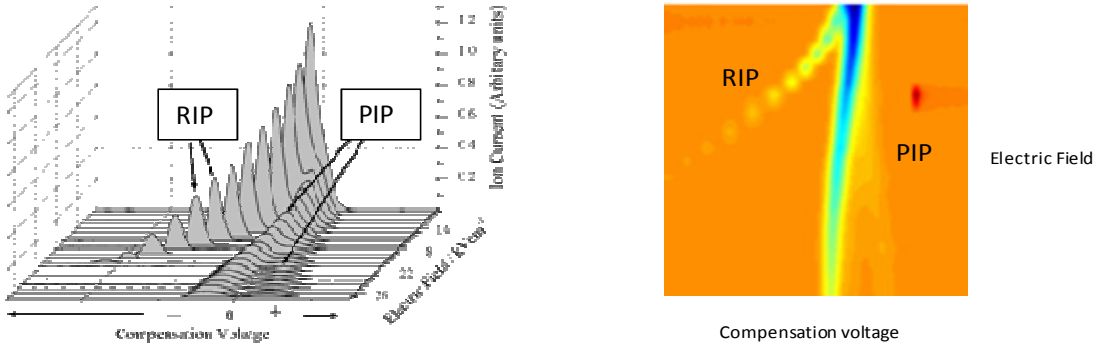

Figure 19 Two different examples of FAIMS dispersion field matrices with the same reactive ion peaks (RIP) and product ion peaks (PIP). In the waterfall plot on the left, the z axis is the ion current; this is replaced in the right, more frequently used, colorplot by color contours

With these data-rich DF matrices a chemical fingerprint is formed, in which identification parameters for different chemical species can be extracted, processed and stored. Figure 17 shows one example: here the CV value at the peak maximum at each of the different electric field settings has been extracted and plotted, to be later used as a reference to identify the same chemicals. In Figure 18a new sample spectrum has been compared to the reference spectrum and clear differences in both spectra can be seen.

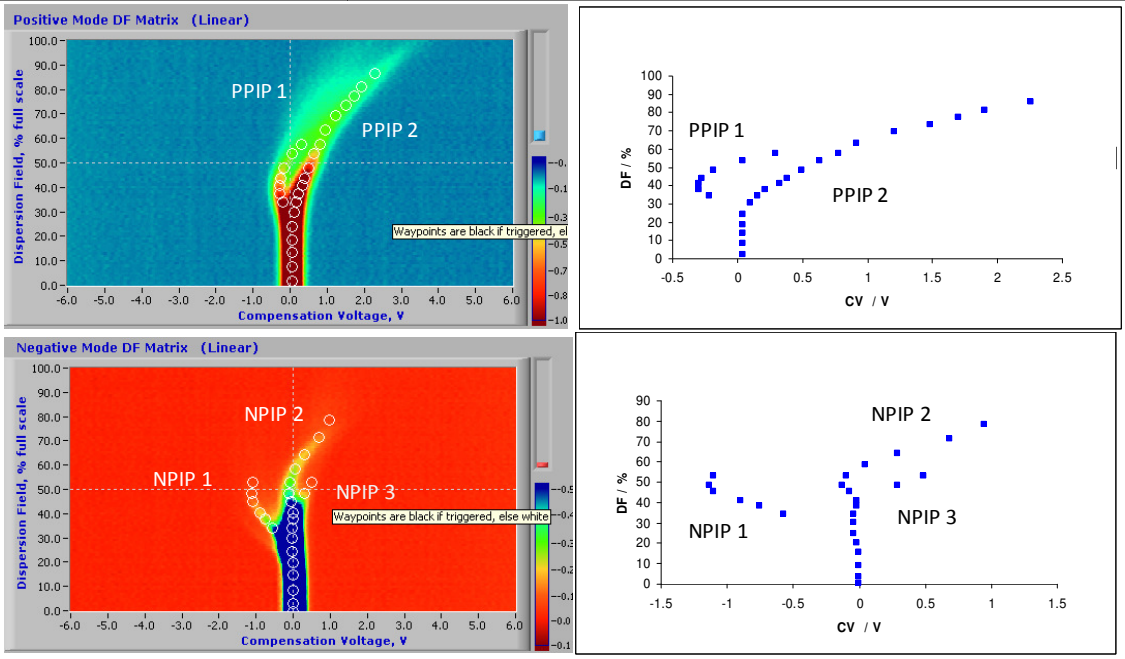

Figure 20 On the left are examples of positive (blue) and negative (red) mode DF matrices recorded at the same time while a sample was introduced into the FAIMS detector. The sample contained 5 chemical species, which showed as two positive product ion peaks (PPIP) and three negative product ion peaks (NPIP). On the right, the CV at the PIP's peak maximum is plotted against % dispersion field to be stored as a spectral reference for subsequent samples.

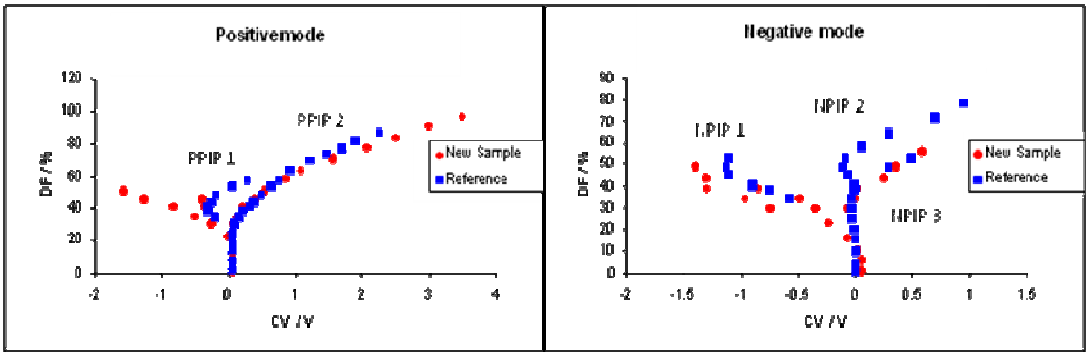

Figure 21 Comparison of two new DF plots with the reference from Figure 10. It can be seen that in both positive and negative modes there are differences between the reference product ion peaks and the new samples